Naval Research Laboratory
Washington, DC 20375-5000

NRL Report 9349

Contributions to Radar Tracking Errors for a Two-point Target Caused by Geometric Approximations

ERIC L. MOKOLE

Target Characteristics Branch
Radar Division

September 19, 1991

Approved for public release; distribution unlimited.

REPORT DOCUMENTATION PAGE

Form Approved
OMB No 0704-0188

1. AGENCY USE ONLY (Leave blank)	2. REPORT DATE	3. REPORT TYPE AND DATES COVERED
	September 19, 1991	Final 1989 - 1991

4. TITLE AND SUBTITLE
Contributions to Radar Tracking Errors for a Two-point Target Caused by Geometric Approximations

5. FUNDING NUMBERS
PE - 61153N
PR - 021-05-43
WU - DN480-006

6. AUTHOR(S)
Eric L. Mokole

7. PERFORMING ORGANIZATION NAME(S) AND ADDRESS(ES)
Naval Research Laboratory
4555 Overlook Avenue, S.W.
Washington, DC 20375-5000

8. PERFORMING ORGANIZATION REPORT NUMBER

9. SPONSORING/MONITORING AGENCY NAME(S) AND ADDRESS(ES)
Office of Naval Research
Arlington, Virginia 22217

10. SPONSORING/MONITORING AGENCY REPORT NUMBER

11. SUPPLEMENTARY NOTES

12a. DISTRIBUTION/AVAILABILITY STATEMENT
Approved for public release; distribution unlimited.

12b. DISTRIBUTION CODE

13. ABSTRACT *(Maximum 200 words)*

Expressions for the exact range and angular errors between the apparent (measured) and actual locations of a two-point target are obtained. The differences between the exact errors and two distinct sets of approximations to them are examined as a function of the ratio of the distance separating the two scattering centers to the actual distance from a monostatic radar to the centroid of the scatterers. One set of approximations to the errors is found in the literature and is apparently the far-field supposition of parallel line propagation paths between points on the target and the radar's aperture. The other set results from expanding appropriate parts of the exact errors in infinite series about the aforementioned ratio and then truncating the various series. The advantages and shortcomings of each set of approximations are identified. The exact expression for the angular error is shown to reduce to both approximations when certain assumptions are made; however, such is not the case for the transverse and radial range errors.

14. SUBJECT TERMS		15. NUMBER OF PAGES
Glint Tracking errors	Two-point target	28 16. PRICE CODE

17. SECURITY CLASSIFICATION OF REPORT	18. SECURITY CLASSIFICATION OF THIS PAGE	19. SECURITY CLASSIFICATION OF ABSTRACT	20. LIMITATION OF ABSTRACT
UNCLASSIFIED	UNCLASSIFIED	UNCLASSIFIED	SAR

CONTENTS

1. INTRODUCTION 1

2. DEFINITIONS 1

3. EXACT CHARACTERIZATION OF RANGE AND ANGULAR ERRORS 2

4. APPROXIMATIONS TO THE EXACT EXPRESSIONS 7

5. EXAMPLES 10

6. LIMITS OF THE RATIO OF THE RANGE ERRORS 20

7. SUMMARY 23

8. REFERENCES 23

CONTRIBUTIONS TO RADAR TRACKING ERRORS FOR A TWO-POINT TARGET CAUSED BY GEOMETRIC APPROXIMATIONS

1. INTRODUCTION

In tracking an extended radar target, an accurate measurement of the target's position is essential. A target is extended [1, p.1] if "its size is sufficient to cause glint errors which exceed the other errors of the system." However the composite signal at the receiver induced by the scattering elements comprising such targets can cause substantial measurement errors of position [1,2,3]. Therefore accurate characterizations of the measured (apparent) range and angular errors of extended targets are important. In Ref. 1 [Ch. 1], these errors are quantified for a two-point target, but an error is introduced by approximating the range to the centroid of the two-point target. Since the accuracy of the characterization has practical significance for radar systems in terms of observed glint errors, this issue is investigated for the ideal situation of a two-point target in a two-dimensional geometry to gain further insight into this problem. Exact expressions of the range and angular errors and an alternate set of approximations to them are derived. Both sets of approximations are compared to the exact errors. These errors depend on the phase (ψ's) of the composite signal, on the differences between the distances from the radar to the two scattering centers and the centroid of the target, and on the relative size of the amplitudes of the individual scattered fields from each center (E_1/E_2).

The alternate approximations are obtained first by expanding appropriate parts of the errors in infinite series and then by truncating the series. The truncated series are polynomials in the ratio of the distance separating the two scattering elements to the actual distance from a radar to the centroid of the scatterers. The differences between the exact errors and the two distinct sets of approximations to them are examined as a function of this ratio. Advantages and shortcomings of each set of approximations are identified. The exact expression for the angular error is shown to reduce both to the first-order approximation and to the expression of Ref. 1 [Ch. 1], when certain approximations are made; however, such is not the case for the transverse and radial range errors.

First the problem is defined, the geometry is specified, and exact expressions for the range and angular errors are derived. This is followed by a discussion of the approximations to the errors and by an analysis of the impact of the approximations relative to the exact expressions for two examples. In particular, limits of the ratios of the different range errors are analyzed in detail. An X-band system (10 GHz) and a large aircraft, which is characterized by a separation of 50 m between the scattering centers, are assumed in both examples. The examples represent an aircraft that is in its landing approach or at a range of roughly 200 nmi.

2. DEFINITIONS

To have consistent terminology, the following definitions are extracted from Ref. 1 and summarized. In keeping with the definition of an extended target, partition the target's surface by subdividing the associated volume with a fine, three-dimensional grid. When the radar observes the target, each small surface element contributes to the total received signal. Those elements that produce strong scatter are called *specular* points [4]. Usually a target has many specular points. An individual point contributes randomly to the echo signal's amplitude and to the apparent position of the extended target, which varies according to the relative motion between the physical target and the radar. Consequently, "a specular point is not any particular geometric point on the surface of the extended target;" rather it "represents a combination of scattering elements which return a

Manuscript approved 8 August 1991

Gaussian signal. Other specular points are similarly composed, and their signals are statistically independent [5,6]."

"Hence, a mathematical model of the extended target must meet two requirements: (a) it must take into account the physical processes which affect radar tracking of the target's extended features, and (b) it must yield results which predict accurately the practical performance of the tracking radar. One such model, the n-point model [7], represents the target as the sum of a large number of random, independent specular points, filling the space occupied by the target." An n-point target model consists of n specular points that can be either independent isotropically reflecting point targets, independent complex reflecting objects, a combination of the two, or any of the preceding where a statistical correlation exists between the scattering centers.

"The number of specular points used to represent the target...may be reduced to a small value for practical purposes, and in some cases the two-point model is used" [2,8,9]. This analysis is undertaken for a two-point target, but may have implications for a more complicated extended target.

3. EXACT CHARACTERIZATION OF RANGE AND ANGULAR ERRORS

Initially the bistatic case is treated, from which the more prevalent, monostatic situation is obtained as a special case. These geometries are depicted in Figs. 1 and 2. The formulation of Ref. 10 is followed. In particular, the origin of the inertial frame is chosen to be the location of the transmitter. In Fig. 1, P_1 and P_2 are the positions of the scattering centers at a given instant of time, O' is the midpoint of the line segment $\overline{P_1P_2}$ whose length is l, P_o is the observation point (location of the receiver) of the scattered field, $\bar{r}_{01}$ and $\bar{r}_{02}$ are the position vectors from the origin to points P_1 and P_2, respectively, and $\bar{r}_1$ and $\bar{r}_2$ are the vectors from P_1 to P_o and P_2 to P_o, respectively. For the sake of argument, assume the magnitudes of $\bar{r}_1$ and $\bar{r}_{01}$ are respectively less than the magnitudes of $\bar{r}_2$ and $\bar{r}_{02}$; that is, $r_1 < r_2$ and $r_{01} < r_{02}$.

The scattered electric field at P_o due to the ith specular point has the form $E_i\cos[\omega(t-t_i)+\delta_i]$ for $i \in \{1,2\}$, where ω is the angular carrier frequency, δ_i is the phase induced by the ith scatterer, t_i is the time delay at P_o over the path from O to P_i to P_o, and E_i is the amplitude of the ith scattering center and is proportional to the square root of its effective radar cross-section. This interpretation of δ_i agrees with that of Ref. 11 [Eq. (71)]. Under the assumption that the polarizations from P_1 and P_2 are identical, the composite signal received at point P_o and time t is

$$e_S(t) = e_1(t) + e_2(t) = E_1\cos[\omega(t-t_1)+\delta_1] + E_2\cos[\omega(t-t_2)+\delta_2] = E_S\cos(\omega t - \psi_S), \quad (1)$$

for the individual fields e_1 and e_2. The composite phase and amplitude are ψ_S and E_S, which after some algebra can be written as

$$E_S = \begin{cases} \sqrt{E_1^2 + E_2^2 + 2E_1E_2\cos(\delta_1 - \delta_2 + \psi)}, & \text{for } E_1 \neq E_2 \\ 2E_1\left[1 + \cos(\delta_1 - \delta_2 + \psi)\right], & \text{for } E_1 = E_2, \text{ and} \end{cases} \quad (2(a))$$

$$\psi_S = \beta + \Phi, \quad (2(b))$$

where

$$\psi = \omega(t_2 - t_1), \tag{3(a)}$$

$$\beta = \omega(t_2 + t_1)/2, \tag{3(b)}$$

$$t_i = (r_i + r_{0i})/c, \tag{3(c)}$$

$$\tan\Phi = \begin{cases} -\dfrac{E_1 \sin\left(\delta_1 + \frac{\psi}{2}\right) + E_2 \sin\left(\delta_2 - \frac{\psi}{2}\right)}{E_1 \cos\left(\delta_1 + \frac{\psi}{2}\right) + E_2 \cos\left(\delta_2 - \frac{\psi}{2}\right)}, & \text{for } E_1 \neq E_2 \\ -\tan\left(\frac{\delta_1 + \delta_2}{2}\right), & \text{for } E_1 = E_2, \end{cases} \tag{3(d)}$$

and c is the speed of light in free space.

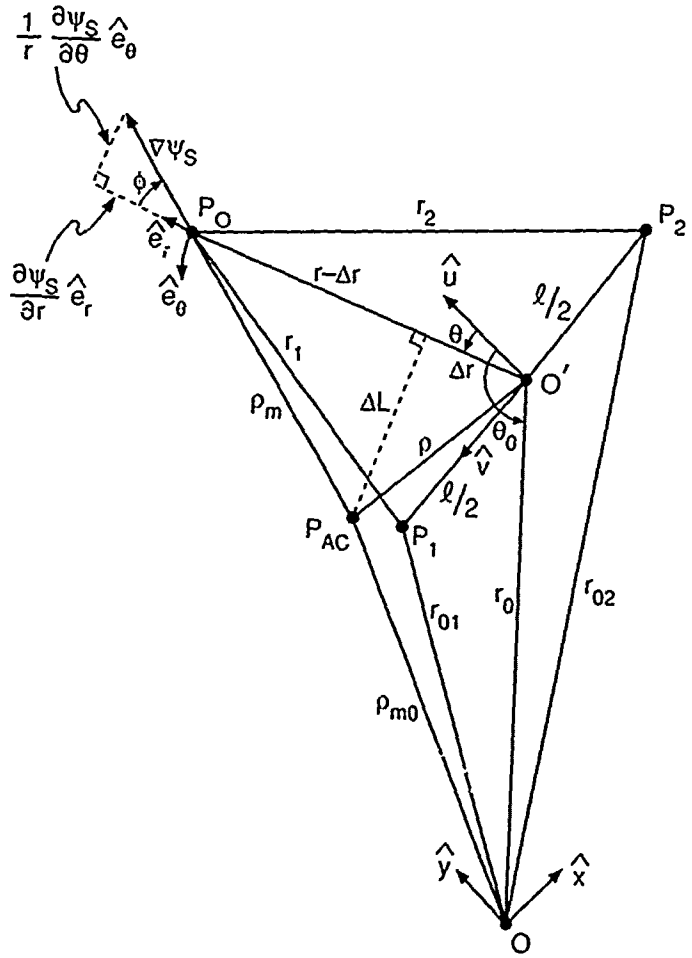

Fig. 1 – Bistatic geometry, where the observation point P_O and the transmitter O are distinct

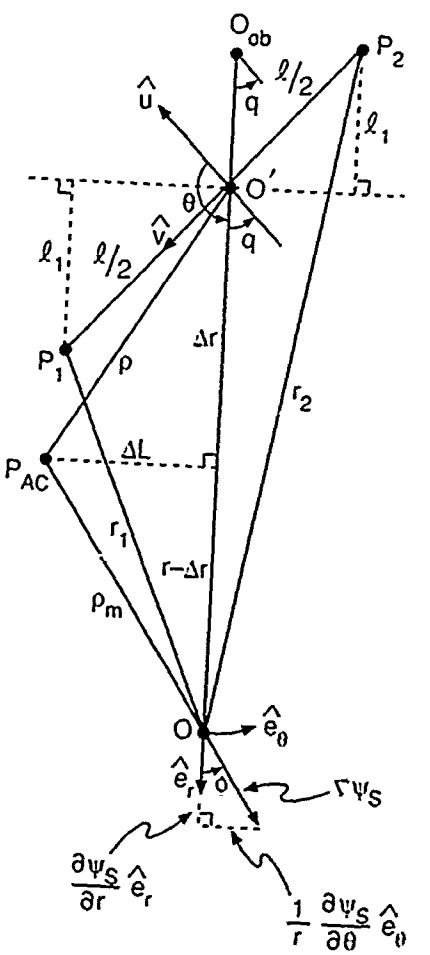

Fig. 2 – Monostatic geometry, where the observation point P_O and the source O are collocated

The expressions for Eq.(2) are obtained by substituting the identities, $\delta_1 - \omega t_1 = \delta_1 - \beta - \psi/2$ and $\delta_2 - \omega t_2 = \delta_2 - \beta + \psi/2$, into Eq.(1) and simplifying the resulting equations. Clearly ψ_S depends on ω, r_1, r_2, r_{01}, r_{02}, δ_1, and δ_2. To simplify subsequent equations, the following definitions of real-valued scalars are used

$$r_a = \frac{r_1 + r_2}{2}, \quad r_{a0} = \frac{r_{01} + r_{02}}{2}, \quad \delta r = r_2 - r_1, \quad \delta r_0 = r_{02} - r_{01}, \quad D = \delta r + \delta r_0. \tag{4}$$

Rewriting β and ψ in this nomenclature leads to

$$\beta = \frac{\omega}{c}(r_a + r_{a0}) \qquad \text{and} \qquad \psi = \frac{\omega}{c}(\delta r + \delta r_0). \tag{5}$$

As a result of various errors, the location of the target measured by a tracking radar is not necessarily any of the points P_1, P_2, or O. Let the location of the measured centroid be denoted P_{AC}, with associated vectors $\overline{\rho}_m$ and $\overline{\rho}_{m0}$ and magnitudes ρ_m and ρ_{m0} from P_{AC} to P_o and O to P_{AC}, respectively (Fig. 1). According to propagation theory [12, pp. 224-227] and experimental measurements [3], the apparent center P_{AC} is determined from the phase ψ_S of the composite signal; that is, the direction of $\overline{\rho}_m$ is the direction of the gradient of ψ_S evaluated at P_o, while its magnitude is specified by

$$\rho_m = \frac{c}{2}\frac{\partial \psi_S}{\partial \omega}\Big|_{P_o},$$

where the partial derivative is the group time delay. Exact expressions for these two quantities are now derived.

First observe that

$$\frac{\partial \psi_S}{\partial \omega} = \begin{cases} \frac{1}{c}\left(r_a + r_{a0}\right) + \frac{\partial \Phi}{\partial \omega}, & \text{for } E_1 \neq E_2 \\ \frac{1}{c}\left(r_a + r_{a0}\right), & \text{for } E_1 = E_2. \end{cases} \tag{6}$$

When E_i and δ_i are constant for the range of frequencies under consideration, this equation simplifies to

$$\frac{\partial \psi_S}{\partial \omega} = \begin{cases} \frac{\left(r_a + r_{a0}\right)}{c} + \frac{D}{c}\frac{E_2^2 - E_1^2}{E_1^2 + E_2^2 + 2E_1E_2\cos(\delta_2 - \delta_1 - \psi)}, & \text{for } E_1 \neq E_2 \\ \frac{\left(r_a + r_{a0}\right)}{c}, & \text{for } E_1 = E_2. \end{cases} \tag{7}$$

Since this analysis takes place in the plane determined by the points O, P_1, and P_2, the gradient depends on two spatial variables. A natural choice is the set of polar coordinates (r, θ) relative to the uv-coordinate frame, whose origin is located at O' with the positive u-axis perpendicular to $\overline{P_1P_2}$ and the positive v-axis coinciding with $\overline{O'P_1}$ (Fig. 1). Therefore the gradient $\nabla\psi_S$ evaluated at P_o is

$$\nabla\psi_S\Big|_{P_o} = \left[\frac{\partial \psi_S}{\partial r}\hat{\mathbf{e}}_r + \frac{1}{r}\frac{\partial \psi_S}{\partial \theta}\hat{\mathbf{e}}_\theta\right]_{P_o}, \tag{8}$$

where $\hat{\mathbf{e}}_r$ and $\hat{\mathbf{e}}_\theta$ are the polar unit vectors. Let (r_0, θ_0) and (r, θ) represent the polar coordinates of the points O and P_o, respectively, and let $\overline{\mathbf{r}}_0$ and $\overline{\mathbf{r}}$ be the associated position vectors from O' with magnitudes r_0 and r.

Before calculating $\nabla\psi_S$, the functional relationships between r_a, r_{a0}, δr, δr_0 and r, θ, r_0, θ_0 are determined. Assuming r_i and r_{0i} are greater than $l/2$ and applying basic trigonometry leads to

$$r_{01} = \sqrt{r_0^2 - r_0 l\sin\theta_0 + l^2/4}, \tag{9(a)}$$

$$r_{02} = \sqrt{r_0^2 + r_0 l\sin\theta_0 + l^2/4}, \tag{9(b)}$$

$$r_1 = \sqrt{r^2 - rl\sin\theta + l^2/4}, \tag{9(c)}$$

$$r_2 = \sqrt{r^2 + rl\sin\theta + l^2/4}, \tag{9(d)}$$

which express the distances r_{01}, r_{02}, r_1, r_2 in terms of the polar variables r, θ, r_0, θ_0. Substitute these expressions into Eq. (4) to get

$$r_{a0} = \frac{1}{2}\left(\sqrt{r_0^2 - r_0 l\sin\theta_0 + l^2/4} + \sqrt{r_0^2 + r_0 l\sin\theta_0 + l^2/4}\,\right), \tag{10(a)}$$

$$r_a = \frac{1}{2}\left(\sqrt{r^2 - rl\sin\theta + l^2/4} + \sqrt{r^2 + rl\sin\theta + l^2/4}\right), \tag{10(b)}$$

$$\delta r_0 = \sqrt{r_0^2 + r_0 l\sin\theta_0 + l^2/4} - \sqrt{r_0^2 - r_0 l\sin\theta_0 + l^2/4}, \tag{10(c)}$$

$$\delta r = \sqrt{r^2 + rl\sin\theta + l^2/4} - \sqrt{r^2 - rl\sin\theta + l^2/4}. \tag{10(d)}$$

Replace the appropriate quantities of Eq. (2(b)) by the preceding expressions to obtain

$$\psi_S = \begin{cases} \frac{\omega}{c}\left(r_a + r_{a0}\right) + \arctan\left\{-\dfrac{E_1\sin\left[\delta_1 + \frac{\omega}{2c}(\delta r + \delta r_0)\right] + E_2\sin\left[\delta_2 - \frac{\omega}{2c}(\delta r + \delta r_0)\right]}{E_1\cos\left[\delta_1 + \frac{\omega}{2c}(\delta r + \delta r_0)\right] + E_2\cos\left[\delta_2 - \frac{\omega}{2c}(\delta r + \delta r_0)\right]}\right\}, & \text{for } E_1 \neq E_2 \\ \frac{\omega}{c}\left(r_a + r_{a0}\right) + \arctan\left\{-\dfrac{\sin\left[\delta_1 + \frac{\omega}{2c}(\delta r + \delta r_0)\right] + \sin\left[\delta_2 - \frac{\omega}{2c}(\delta r + \delta r_0)\right]}{\cos\left[\delta_1 + \frac{\omega}{2c}(\delta r + \delta r_0)\right] + \cos\left[\delta_2 - \frac{\omega}{2c}(\delta r + \delta r_0)\right]}\right\}, & \text{for } E_1 = E_2. \end{cases} \tag{11}$$

As a brief aside, note that ψ_S clearly depends on the carrier ω, E_1/E_2, $r_1 + r_2$, and $r_1 - r_2$. Now taking the partial derivatives indicated in Eq. (8) and making some minor algebraic adjustments yield

$$\left.\frac{\partial\psi_S}{\partial r}\right|_{P_0} = \frac{\omega}{4c}\left\{\frac{2r + l\sin\theta}{\sqrt{r^2 + rl\sin\theta + l^2/4}} + \frac{2r - l\sin\theta}{\sqrt{r^2 - rl\sin\theta + l^2/4}} + \left(\frac{2r + l\sin\theta}{\sqrt{r^2 + rl\sin\theta + l^2/4}} - \frac{2r - l\sin\theta}{\sqrt{r^2 - rl\sin\theta + l^2/4}}\right) \times \frac{E_2^2 - E_1^2}{E_1^2 + E_2^2 + 2E_1E_2\cos\left[\delta_2 - \delta_1 - (\delta r + \delta r_0)\omega/c\right]}\right\}, \tag{12(a)}$$

$$\left.\frac{1}{r}\frac{\partial\psi_S}{\partial r}\right|_{P_0} = \frac{\omega}{4c}\left\{\frac{l\cos\theta}{\sqrt{r^2 + rl\sin\theta + l^2/4}} - \frac{l\cos\theta}{\sqrt{r^2 - rl\sin\theta + l^2/4}} + \left(\frac{l\cos\theta}{\sqrt{r^2 + rl\sin\theta + l^2/4}} + \frac{l\cos\theta}{\sqrt{r^2 - rl\sin\theta + l^2/4}}\right) \times \frac{E_2^2 - E_1^2}{E_1^2 + E_2^2 + 2E_1E_2\cos\left[\delta_2 - \delta_1 - (\delta r + \delta r_0)\omega/c\right]}\right\}, \tag{12(b)}$$

when $E_1 \neq E_2$. If $E_1 = E_2$, the expressions for the partial derivatives are obtained from Eqs. (12(a)) and (12(b)) by omitting the product terms so that only the first two terms remain for each partial.

The angular error between the measured (apparent) and actual locations of the target is the angle from $\hat{\mathbf{e}}_r$ to $\nabla\psi_S$ in the counterclockwise direction. In the geometry of Fig. 1, ϕ is an acute, negative angle and

$$\tan\phi = \frac{1}{r}\frac{\partial\psi_S}{\partial\theta} \Big/ \frac{\partial\psi_S}{\partial r}. \tag{13}$$

No standard definition of a formula to represent the range error currently exists. However two natural candidates are the radial range error R_e and the magnitude ρ of the vector error $(\bar{r} - \bar{\rho}_m)$, which are given by

$$R_e = r - \rho_m = |\bar{r}| - |\bar{\rho}_m| \quad \text{and} \quad \rho = |\bar{\rho}| = |\bar{r} - \bar{\rho}_m|. \tag{14}$$

A third choice is the range error projected along the actual direction

$$\Delta r = r - \left|\text{Projection of } \bar{\rho}_m \text{ onto } \bar{r}\right| = r - \rho_m \cos\phi. \tag{15}$$

It is clear from the geometry of Fig. 1 that relationships among these errors exist. If a fourth error $(\Delta L = \rho_m \sin\phi)$, the error in the direction transverse to $\bar{r}$, is defined, these relationships may be quantified. In particular, Δr and ΔL are the orthogonal components of $\bar{\rho}$. Since

$$\rho^2 = (\Delta r)^2 + (\Delta L)^2 = R_e^2 + 4r\rho_m \sin^2(\phi/2), \tag{16}$$

ρ is clearly the largest error. Observe that

$$R_e = \begin{cases} r - \frac{r_a + r_{a0}}{2} - \frac{D}{2}\frac{E_2^2 - E_1^2}{E_1^2 + E_2^2 + 2E_1E_2\cos\left[\delta_2 - \delta_1 - 2\omega\delta r/c\right]}, & \text{for } E_1 \neq E_2 \\ r - \frac{r_a + r_{a0}}{2}, & \text{for } E_1 = E_2 \end{cases} \tag{17}$$

is the only error independent of ϕ and that ρ and $|\Delta r|$ approach $|R_e|$ in the limit as ϕ approaches zero.

In analyzing expressions for the errors, it is useful to introduce three new parameters,

$$\gamma_0 = \frac{l}{r_0}, \qquad \gamma = \frac{l}{r}, \qquad z_0 = \frac{E_1}{E_2}, \tag{18}$$

the first two of which are numbers between zero and one for this application. Although the equations for the errors of the bistatic case can be reformulated in terms of γ_0, γ, and z_0, the monostatic case is treated instead because it has greater applicability to radar scenarios, not to mention that the calculations are much less cumbersome. Results for monostatic tracking radars are obtained by setting

$$r = r_0, \quad r_a = r_{a0}, \quad \theta = \theta_0, \quad \hat{\mathbf{e}}_r = \hat{\mathbf{e}}_{r_0}, \quad \hat{\mathbf{e}}_\theta = \hat{\mathbf{e}}_{\theta_0}, \quad \delta r = \delta r_0, \quad \phi = \phi_0, \quad \gamma = \gamma_0, \tag{19}$$

and the corresponding geometry (Fig. 2) is obtained by letting the point P_o coincide with O.

Therefore in the monostatic case for $z_0 \neq 1$, the expressions for ψ_S and the various errors become

$$\tan\phi = \frac{\gamma\cos\theta}{2}\left\{-\frac{\delta r}{r} + \frac{2r_a}{r}\frac{1-z_0^2}{z_0^2+1+2z_0\cos[\delta_2-\delta_1-2\omega\delta r/c]}\right\}$$
$$\div\left\{\frac{2r_a}{r} - \frac{\gamma}{2}\sin\theta\frac{\delta r}{r} + \left(\frac{\delta r}{r} + \frac{\gamma}{2}\sin\theta\frac{2r_a}{r}\right)\right.$$
$$\left.\times\frac{1-z_0^2}{z_0^2+1+2z_0\cos[\delta_2-\delta_1-2\omega\delta r/c]}\right\}, \tag{20(a)}$$

$$R_e = r - r_a - \delta r\frac{1-z_0^2}{z_0^2+1+2z_0\cos[\delta_2-\delta_1-2\omega\delta r/c]}, \tag{20(b)}$$

$$\Delta r = r - \cos\phi\left\{r_a + \delta r\frac{1-z_0^2}{z_0^2+1+2z_0\cos[\delta_2-\delta_1-2\omega\delta r/c]}\right\}, \tag{20(c)}$$

$$\Delta L = \sin\phi\left\{r_a + \delta r\frac{1-z_0^2}{z_0^2+1+2z_0\cos[\delta_2-\delta_1-2\omega\delta r/c]}\right\}, \tag{20(d)}$$

$$\psi_S = \frac{2\omega r_a}{c} + \arctan\left\{-\frac{\sin[\delta_1+\omega\delta r/c] + z_0\sin[\delta_2-\omega\delta r/c]}{\cos[\delta_1+\omega\delta r/c] + z_0\cos[\delta_2-\omega\delta r/c]}\right\}, \tag{20(e)}$$

while for $z_0 = 1$

$$\tan\phi = \frac{\gamma\cos\theta}{2}\left\{-\frac{\delta r}{r} \div \left(\frac{2r_a}{r} - \frac{\gamma}{2}\sin\theta\frac{\delta r}{r}\right)\right\}, \tag{21(a)}$$

$$R_e = r - r_a, \tag{21(b)}$$

$$\Delta r = r - r_a\cos\phi, \tag{21(c)}$$

$$\Delta L = r_a\sin\phi, \tag{21(d)}$$

$$\psi_S = \frac{2\omega r_a}{c} - \frac{\delta_1+\delta_2}{2}. \tag{21(e)}$$

Clearly Eqs. (21) are directly obtainable from Eqs. (20) by letting z_0 be unity; however, one would not arrive at Eqs. (21) if the argument of the cosine, $\delta_2 - \delta_1 - 2\omega\delta r/c$, is set equal to zero before letting z_0 be zero. When calculating such limits, they must be taken in the proper order. In this problem, the limit with respect to z_0 must be evaluated first. In fact, the double limit obtained by letting $\delta_2 - \delta_1 - 2\omega\delta r/c$ approach zero, followed by z_0 approaching one, does not even exist.

Even though it is assumed that $r_1 < r_2$ and $r_{01} < r_{02}$ (hence $\theta, \theta_0 \in [\pi/2, \pi)$) in the preceding arguments and figures, the results thus far are true for all $\theta, \theta_0 \in [0, 2\pi)$.

4. APPROXIMATIONS TO THE EXACT EXPRESSIONS

The exact expressions of the errors given by Eqs.(20) depend on the parameter γ, which lies in the open interval $(0, 1)$. In particular, an implicit dependence occurs in δr and r_a or, equivalently, in the individual ranges r_1 and r_2. It is further assumed that γ is small enough to guarantee the convergence of the binomial series representations of r_1 and r_2. Consequently,

$$r_1 = r\left\{1 - \frac{\gamma}{2}\sin\theta + \frac{\gamma^2}{8}\cos^2\theta + \frac{\gamma^3}{16}\sin\theta\cos^2\theta + O(\gamma^4)\right\}, \tag{22(a)}$$

$$r_2 = r\left\{1 + \frac{\gamma}{2}\sin\theta + \frac{\gamma^2}{8}\cos^2\theta - \frac{\gamma^3}{16}\sin\theta\cos^2\theta + O(\gamma^4)\right\}, \tag{22(b)}$$

which imply

$$\frac{\delta r}{r} = \gamma \sin\theta - \frac{\gamma^3}{8}\sin\theta\cos^2\theta + O(\gamma^4), \tag{23(a)}$$

$$\frac{r_a}{r} = 1 + \frac{\gamma^2}{8}\cos^2\theta + O(\gamma^4), \tag{23(b)}$$

$$\psi = \frac{2\omega r}{c}\left\{\gamma\sin\theta - \frac{\gamma^3}{8}\sin\theta\cos^2\theta + O(\gamma^4)\right\}. \tag{23(c)}$$

The O-notation means terms of that order and higher.

The preceding three expressions can be approximated by truncating the appropriate infinite series. The least accurate approximations are obtained by eliminating all terms with γ raised to a power greater than or equal to one or two, which are respectively called the zeroth- and first-order approximations and are designated by zero and one subscripts. For example,

$$\tan\phi_1 = \frac{\gamma\cos\theta}{2}\frac{1 - z_0^2}{z_0^2 + 1 + 2z_0\cos\left[\delta_2 - \delta_1 - (2\omega\gamma r/c)\sin\theta\right]}, \tag{24(a)}$$

$$R_{e1} = -l\sin\theta\frac{1 - z_0^2}{z_0^2 + 1 + 2z_0\cos\left[\delta_2 - \delta_1 - (2\omega\gamma r/c)\sin\theta\right]}; \tag{24(b)}$$

$$\Delta r_1 = r - r\cos\phi_1\left\{1 + \gamma\sin\theta\frac{1 - z_0^2}{z_0^2 + 1 + 2z_0\cos\left[\delta_2 - \delta_1 - (2\omega\gamma r/c)\sin\theta\right]}\right\}, \tag{24(c)}$$

$$\Delta L_1 = r\sin\phi_1\left\{1 + \gamma\sin\theta\frac{1 - z_0^2}{z_0^2 + 1 + 2z_0\cos\left[\delta_2 - \delta_1 - (2\omega\gamma r/c)\sin\theta\right]}\right\}. \tag{24(d)}$$

Equations (24) are valid for $z_0 \neq 1$. When $z_0 = 1$, $\tan\phi_1$ and R_{e1} are zero, Δr_1 is $r(1 - \cos\phi_1)$, and ΔL_1 is $r\sin\phi_1$.

Analogous expressions for Eqs. (24) from Ref. 1 [Eqs. (1.11) and (1.14)] are given by

$$\tan\phi_{ob} = -\frac{l\cos q}{2r_a}\frac{1 - z_0^2}{z_0^2 + 1 + 2z_0\cos\left[(2\omega l/c)\sin q\right]}, \tag{25(a)}$$

$$\Delta r_{ob} = -\frac{l\sin q}{2}\frac{1 - z_0^2}{z_0^2 + 1 + 2z_0\cos\left[(2\omega l/c)\sin q\right]}, \tag{25(b)}$$

$$\Delta L_{ob} = -l\cos q\frac{1 - z_0^2}{z_0^2 + 1 + 2z_0\cos\left[(2\omega l/c)\sin q\right]}. \tag{25(c)}$$

To account for the apparent sign errors in the formulae for Φ and ϕ of Ref. 1 [pp. 7,9], minus signs are inserted following the equal signs in Eqs. (25). A similar sign difference is also found in Ref. 10 [p. 1822] in the equivalent expression denoted ψ, on which the result of Ref. 1 is based.

First note that the parameter "r" of Ref. 1 is an approximation to the actual range r. In particular, it is r_a, the average of r_1 and r_2. To make comparisons between the results of Ref. 1 and the exact and approximate expressions of this report, their "r" has been replaced with r_a. Consequently, the center of their moving coordinate axis is situated at O_{ob} at a distance r_a from O (Fig. 2).

Secondly, the directed angle q is measured from the line segment $\overline{O'O}$ to the perpendicular bisector of $\overline{P_1P_2}$ on the O side of $\overline{P_1P_2}$. It is not clear from Refs.1 and 10 how q is defined. So the

aforementioned definition is selected. For the geometry of Fig. 2, q is related to θ by $\theta + q = \pi$. In fact, the relationship between θ and q for arbitrary configurations is given by

$$\theta + q = \begin{cases} 0, & \text{for } 0 \le \theta < \pi/2 \\ \pi, & \text{for } \pi/2 \le \theta < 3\pi/2 \\ 2\pi, & \text{for } 3\pi/2 \le \theta < 2\pi. \end{cases} \tag{26}$$

The authors of Ref. 1 [pp. 4-12] never explicitly state what approximations are used for r_1 and r_2, but they apparently follow the work of Ref. 10, which employs the approximations $r - (l/2)\sin q$ and $r + (l/2)\sin q$, respectively. The geometrical significance of this approximation can be understood by consulting Fig. 2 and observing that $l_1 = (l/2)\sin q$ is the distance of P_1 and P_2 from the line through O' perpendicular to $\bar{r}$. Hence r_1 and r_2 are approximated by their projections onto the line through O and O_{ob}. Although it cannot be stated with absolute certainty, it is likely that their approximation is related to the far-field assumption of parallel lines: the two triads of line segments that connect P_o to O', P_1, P_2 and O to the same three points are approximately parallel. As a final comment, the selection of expressions to represent Δr_{ob} and ΔL_{ob} is disturbing because the choice is independent of ϕ. According to the graphical depiction of Ref. 1 [Fig. 1.3, p. 8], Δr_{ob} and ΔL_{ob} are the radial and perpendicular components of the vector error $\bar{\rho}$. Thus they must depend on the angular error ϕ in the same manner that Eqs. (20(c)), (20(d)), (24(c)), and (24(d)) do, which is in opposition to the analytical definitions attributed to them by Eqs. (25(b)) and (25(c)). Consequently, the respective differences among Δr, ΔL, ρ and Δr_{ob}, ΔL_{ob}, $[(\Delta r_{ob})^2 + (\Delta L_{ob})^2]^{1/2}$ will be examined more closely.

Because they are concerned with an accurate characterization of the range and angular errors, the three approximations ("r," r_1, r_2) that Ref. 1 makes are important. In essence, they introduce an intrinsic error at the outset to all subsequent equations. To ascertain the geometrical effect of substituting r_a for r, solve Eq.(10(b)) for r to obtain

$$r = r_a \sqrt{\frac{4r_a^2 - l^2}{4r_a^2 - l^2\sin^2\theta}}. \tag{27}$$

Clearly, r is a function of the target orientation (θ) to the radar and the extent (l) of the target relative to the average range (r_a) of the two scatterers. Since the numerator of the radicand is less than the denominator, $r < r_a$. Hence, as indicated in Fig. 2, O_{ob} is farther away from O than O'. More importantly, the radicand varies between $\sqrt{1 - (l^2)/(4r_a^2)}$ and 1 for any value of θ. Hence the approximation of r by r_a is only as good as the approximation of 1 by $\sqrt{1 - (l^2)/(4r_a^2)}$.

Substituting $q = \pi - \theta$ into Eqs. (25) yields

$$\tan\phi_{ob} = \frac{l\cos\theta}{2r_a}\frac{1 - z_0^2}{z_0^2 + 1 + 2z_0\cos[(2\omega l/c)\sin\theta]}, \tag{28(a)}$$

$$\Delta r_{ob} = -\frac{l\sin\theta}{2}\frac{1 - z_0^2}{z_0^2 + 1 + 2z_0\cos[(2\omega l/c)\sin\theta]}, \tag{28(b)}$$

$$\Delta L_{ob} = l\cos\theta\frac{1 - z_0^2}{z_0^2 + 1 + 2z_0\cos[(2\omega l/c)\sin\theta]}. \tag{28(c)}$$

Upon identifying r with r_a in Eqs. (28), Eq. (28(a)) is identical to Eq. (24(a)) when $\delta_2 - \delta_1 = 0$; however,

$$\frac{1}{2\cos\phi_1}\left\{\Delta r_1 - r(1 - \cos\phi_1)\right\} \quad \text{and} \quad \frac{-1}{2\sin\phi_1}\left\{\Delta L_1 - r\sin\phi_1\right\} \tag{29}$$

rather than Δr_1 and ΔL_1 agree with Δr_{ob} and ΔL_{ob}. In light of the preceding discussion, the disagreements between Δr_{ob} and Δr_1 and ΔL_{ob} and ΔL_1 are not unexpected. In addition, Eq. (24(a)) is equivalent to Ref. 3 [Eq. (3)] with the identification of $r \tan\phi$, $\delta_2 - \delta_1 - \psi$, l, θ, and z_0 to E, $\phi + L\sin\psi$, L, ψ, and a. Lastly, observe that the only effect of changing the range of θ from $[\pi/2, 3\pi/2)$ to $[0, \pi/2) \cup [3\pi/2, 2\pi)$ is to change the sign for each of Eqs. (28).

5. EXAMPLES

For very small γ, the first-order approximations are very good; however, these results may not be accurate enough for all situations of interest. In addition, it is not clear analytically how good the approximations of Ref. 1 are. Therefore a comparison between the exact and approximate representations of the range and angular errors is now undertaken by considering two examples for $z_0 = 0.5$ and for a carrier frequency of 10 GHz. To represent a large aircraft, the scattering centers are separated by 50 m. Hence, for an aircraft that is landing or one that is 200 nmi from the radar, the respective γs are 0.05 and 0.00025. The examples are treated in that order.

Figures 3(a) through 3(c) indicate that the absolute value of the angular errors of Eqs. (20(a)), (24(a)), and (28(a)) can get up to 0.07 rad (4.0°), which is not insignificant. In fact, the approximations are nearly equal since their difference lies in the interval [-0.00003,0.00003] rad (Fig. 3(b)). The difference between ϕ_{ob} and ϕ (hence between ϕ_1 and ϕ) fluctuates between -0.06 and 0.06 rad (Fig. 3(c)). Since the differences, $\phi - \phi_{ob}$ and $\phi - \phi_1$, can be as large as the actual angular error, neither approximation is good for all ranges of θ.

In terms of the radial range error, Fig. 4(a) shows that $|\Delta r|$ can be 150 m, which is three times the separation between the scattering centers. Since the ratio $|\Delta r/\Delta r_{ob}|$ is often greater than 1 and can be as large as 15 (Fig. 4(b)), $|\Delta r_{ob}|$ could be a mere 10 m, one-fifteenth the actual radial error. Clearly Δr_{ob} is not a good measure of this error and is particularly bad near θ equal 0, π, and 2π, where the graph of $|\Delta r/\Delta r_{ob}|$ appears to blow up. In contrast, Δr_1 is a better approximation of Δr (Fig. 4(c)) roughly by a factor of two for the entire range of θ; but in small intervals about $\pi/2$ and $3\pi/2$, the approximation is excellent.

Figure 5 provides a comparison of the various transverse errors. The absolute value of the actual transverse error can reach 65 m (Fig 5(a)), and $|\Delta L/\Delta L_{ob}|$ can be as high as 4 (Fig. 5(b)). Therefore ΔL_{ob} is not a good estimate of this error. However ΔL_1 is an even poorer approximation of ΔL (Fig. 5(c)) since $\Delta L_1 \simeq 2\Delta L_{ob}$, except for θ near 0, $\pi/2$, π, $3\pi/2$, and 2π, where ΔL_1 is a very good estimate of ΔL.

Since $|\Delta r/\Delta r_{ob}|$ and $|\Delta L/\Delta L_{ob}|$ are as large as 15 and 4, respectively, and the maximum of ρ is 150 m (Fig. 6(a)), one expects the maximum of $\rho/[(\Delta r_{ob})^2 + (\Delta L_{ob})^2]^{1/2}$ to have an upper bound of $150/\sqrt{241} \simeq 9.66$. This expectation is verified by Fig. 6(b), where the maximum value is nearly 7. Therefore $[(\Delta r_{ob})^2 + (\Delta L_{ob})^2]^{1/2}$ is a poor measure of ρ. Similarly, ρ_1 is a poor estimate of ρ except for values of θ centered about 0, $\pi/2$, π, $3\pi/2$, and 2π (Fig. 6(c)).

The preceding example demonstrates that the first-order approximations of Eqs.(24) and the expressions of Ref. 1 can be poor representations of the angular, radial range, and transverse range errors. In such instances, one should rely on the exact errors (Eqs.(20)).

Comparisons of the errors for the second example ($\gamma = 0.00025$) are displayed in Figs. 7 through 10. The range errors (ΔL, Δr, and ρ) have essentially the same form and magnitude as the preceding example, and the angular error ϕ has the same form but is 200 times smaller. However, the behavior of the approximations relative to the errors is significantly different; for example, the symmetry about $\theta = \pi$ may be absent (Figs. 7(c), 8(b), 9(b), 10(c)). In addition, excursions of the first-order approximations from the actual errors are much smaller than those of the first example, and the analytical relationships among the exact errors and both sets of approximations are apparent for small values of γ. In particular, $\phi \simeq \phi_{ob} \simeq \phi_1$, $\Delta r \simeq \Delta r_1 \simeq 2\Delta r_{ob}$,

and $\Delta L \simeq \Delta L_1 \simeq \Delta L_{ob}/2$; and Δr, ΔL, ρ, and ϕ respectively lie in [-150 m,150 m], [-75 m,75 m], [0,150 m], and [-0.5 mrad,0.5 mrad] (see Figs. 7(a) through 10(a)).

Both approximations to the angular error ϕ are excellent. Since ϕ_1 and ϕ_{ob} are indistinguishable up to the twelfth decimal, only $\phi - \phi_{ob}$ is sketched (Fig. 7(c)). This difference gets no larger than 3×10^{-7} rad. The first-order approximations of ΔL, Δr, and ρ are also very good except possibly at θ equal 0, π, and 2π (Figs. 8(c), 9(c), 10(c)). In contrast, the transverse and radial errors of Ref. 1 apparently converge to multiples of the actual errors except possibly near 0, π, and 2π (Figs. 8(b), 9(b)); while $\sqrt{\Delta r_{ob}^2 + \Delta L_{ob}^2}$ smoothly oscillates between one-half and twice the actual error ρ (Fig. 10(b)).

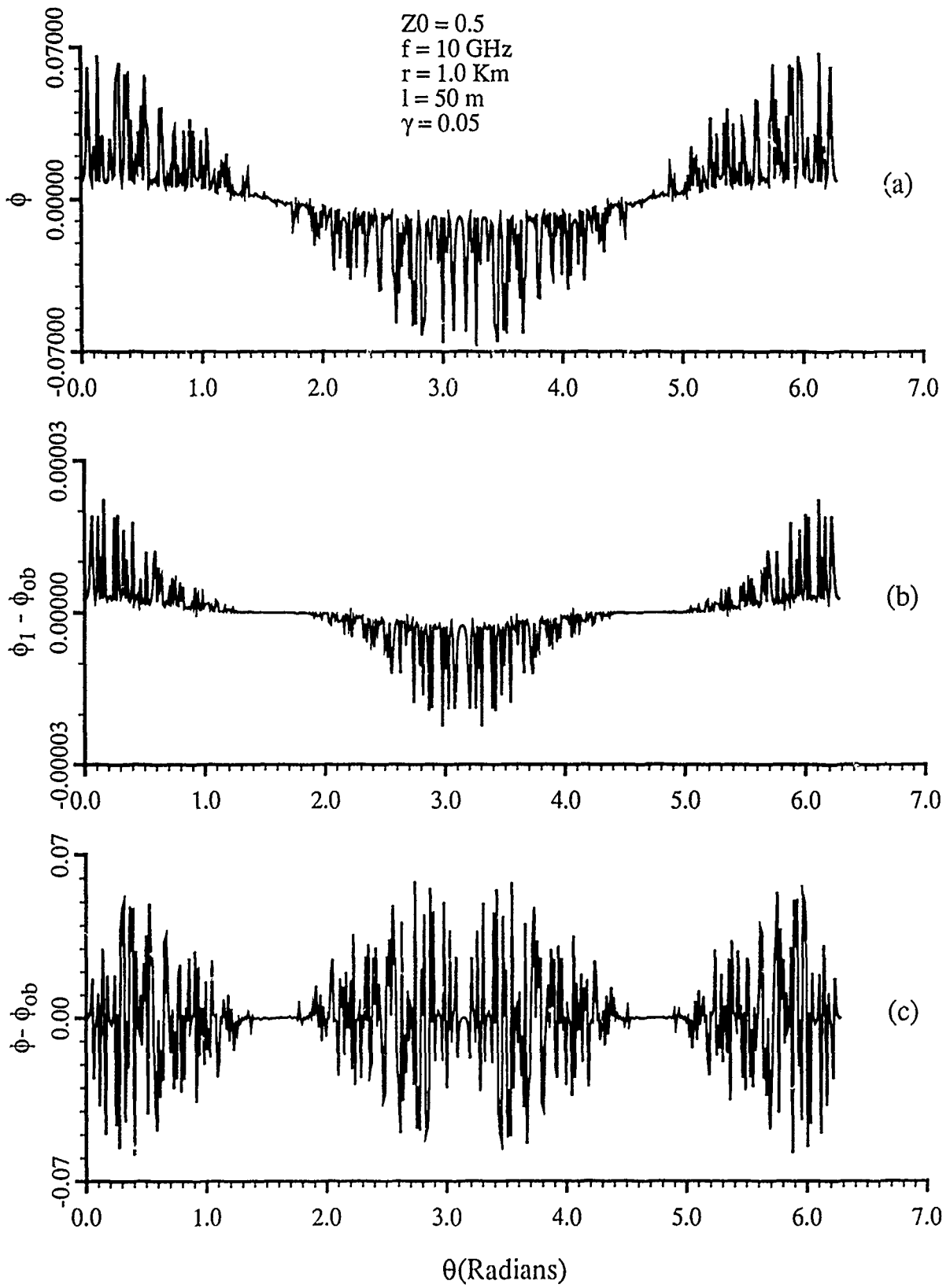

Fig. 3 – Plots of ϕ, $\phi_1 - \phi_{ob}$, and $\phi - \phi_{ob}$ versus θ, all of which are in radians

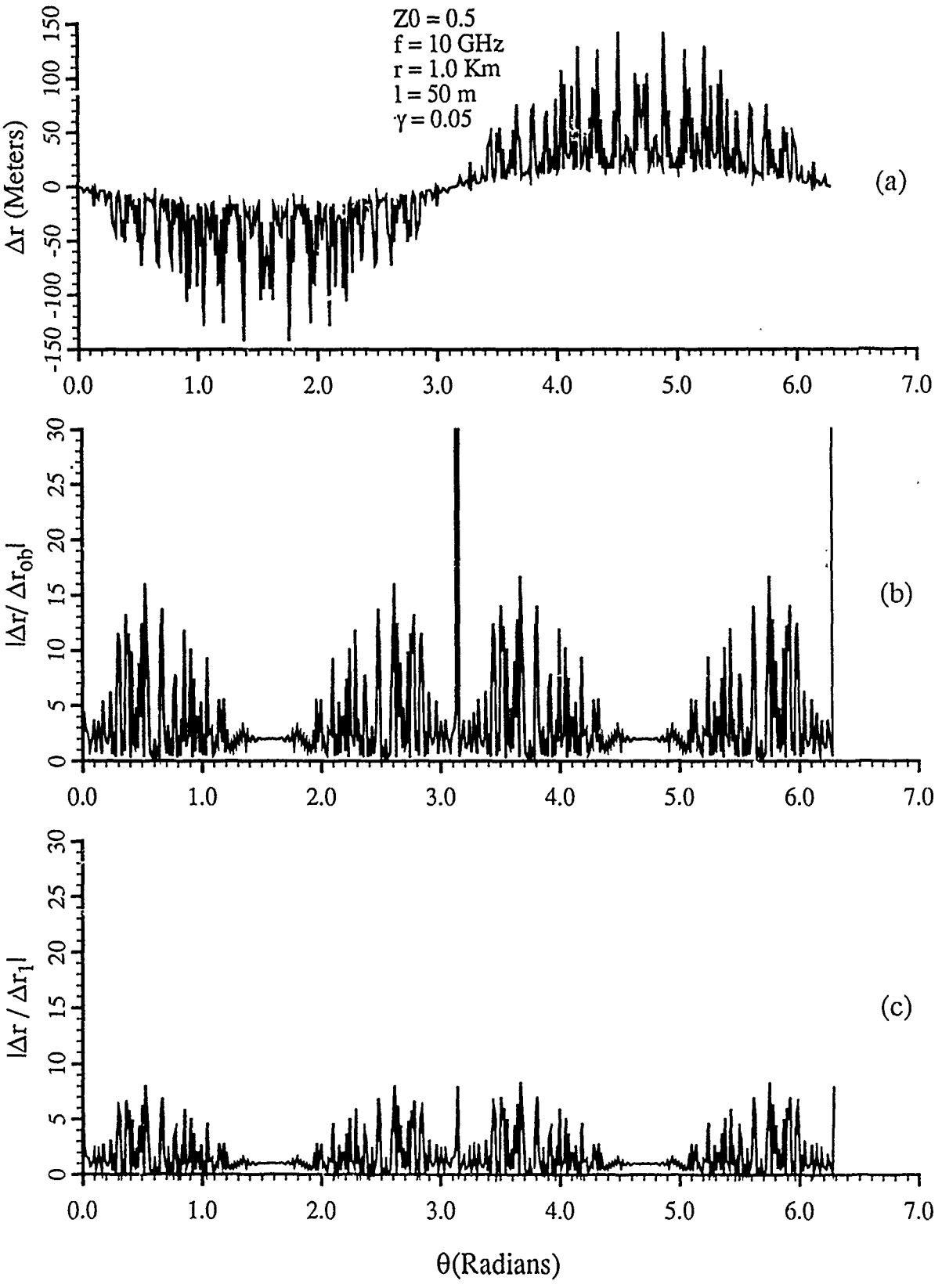

Fig. 4 – Plots of Δr, $|\Delta r / \Delta r_{ob}|$, and $|\Delta r / \Delta r_1|$ versus θ

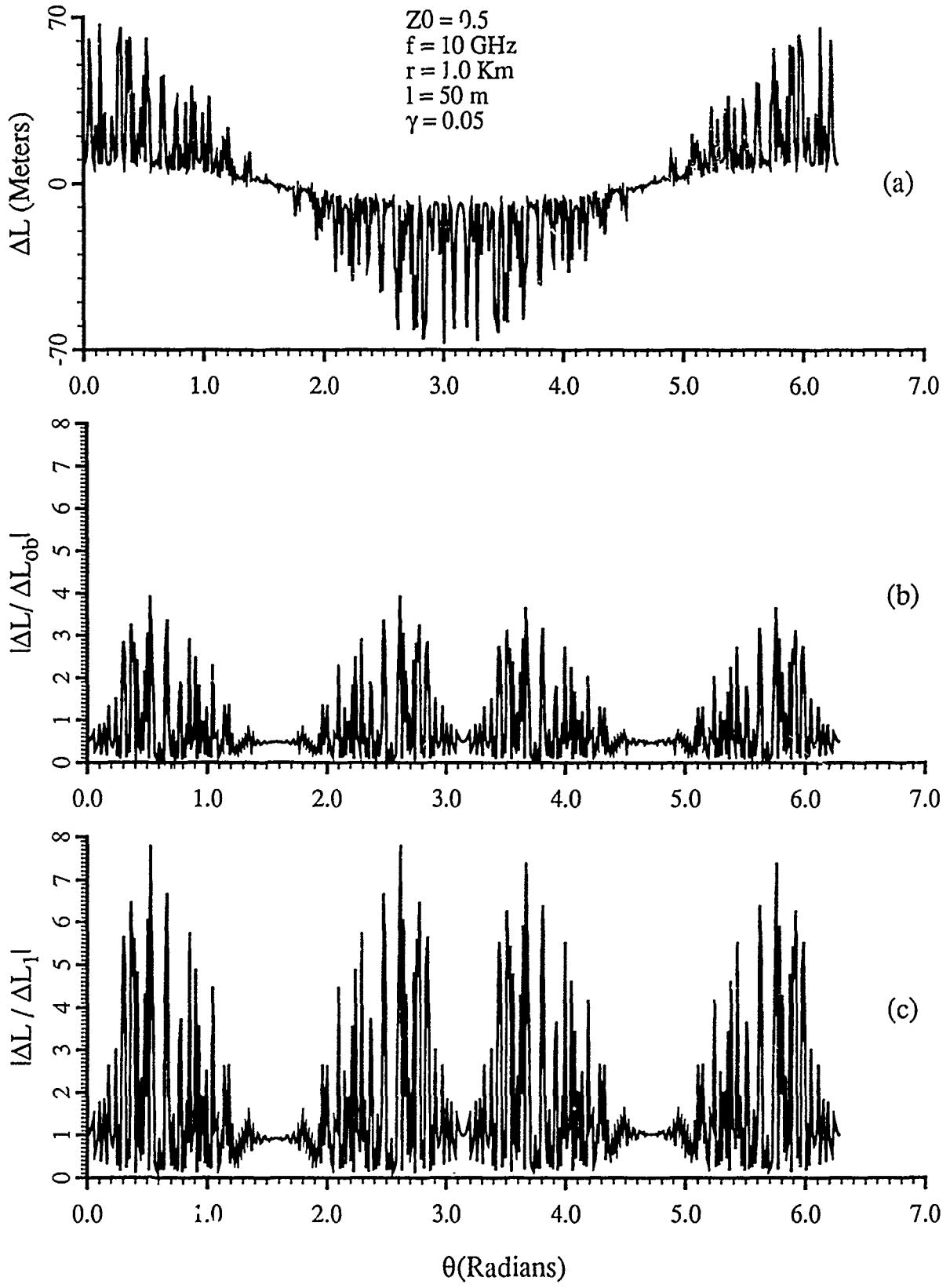

Fig. 5 – Plots of ΔL, $|\Delta L / \Delta L_{ob}|$, and $|\Delta L / \Delta L_1|$ versus θ

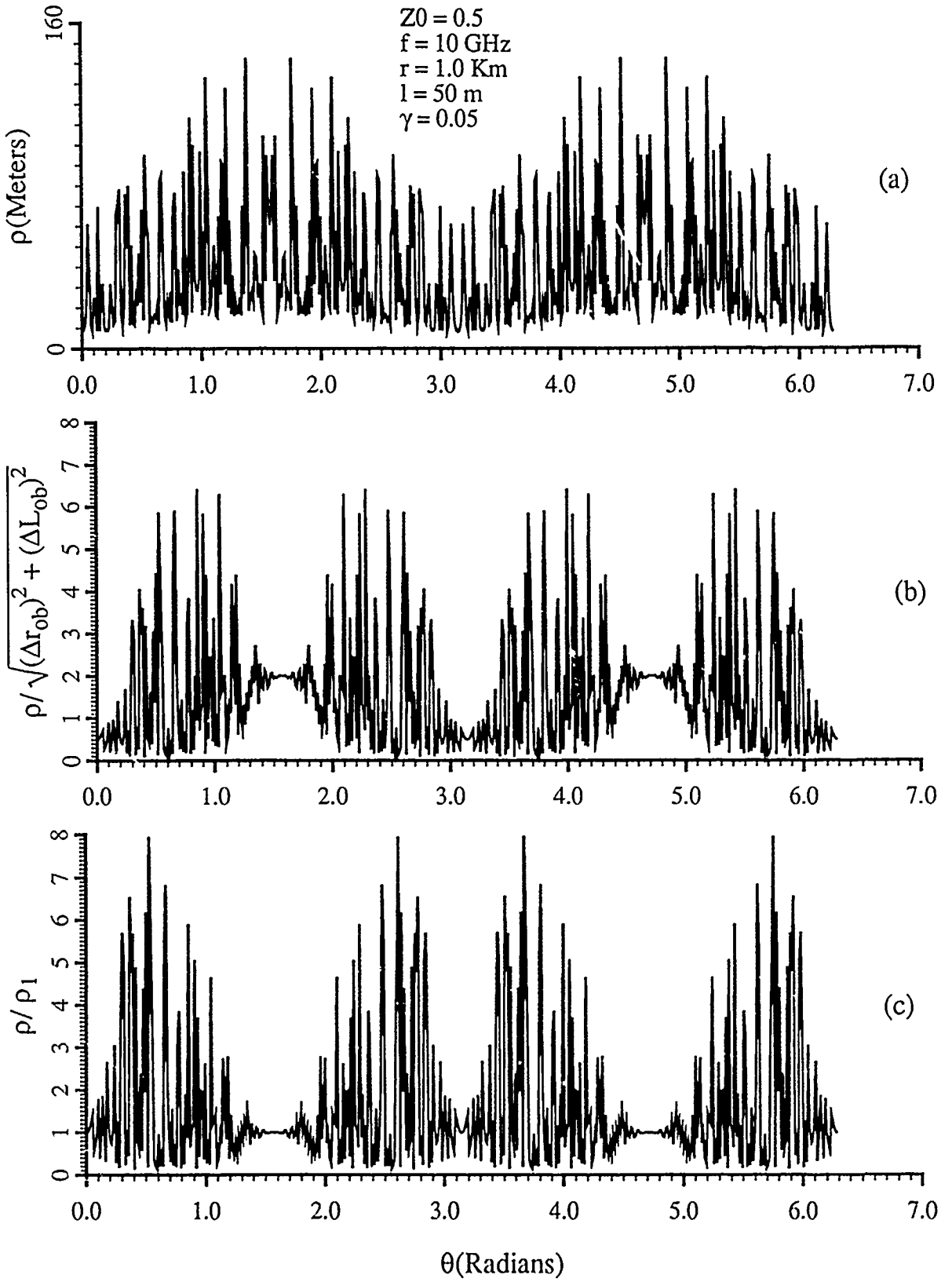

Fig. 6 – Plots of the magnitude of the vector error of the measured position relative to the actual position and of ratios between the magnitude and two approximations to it

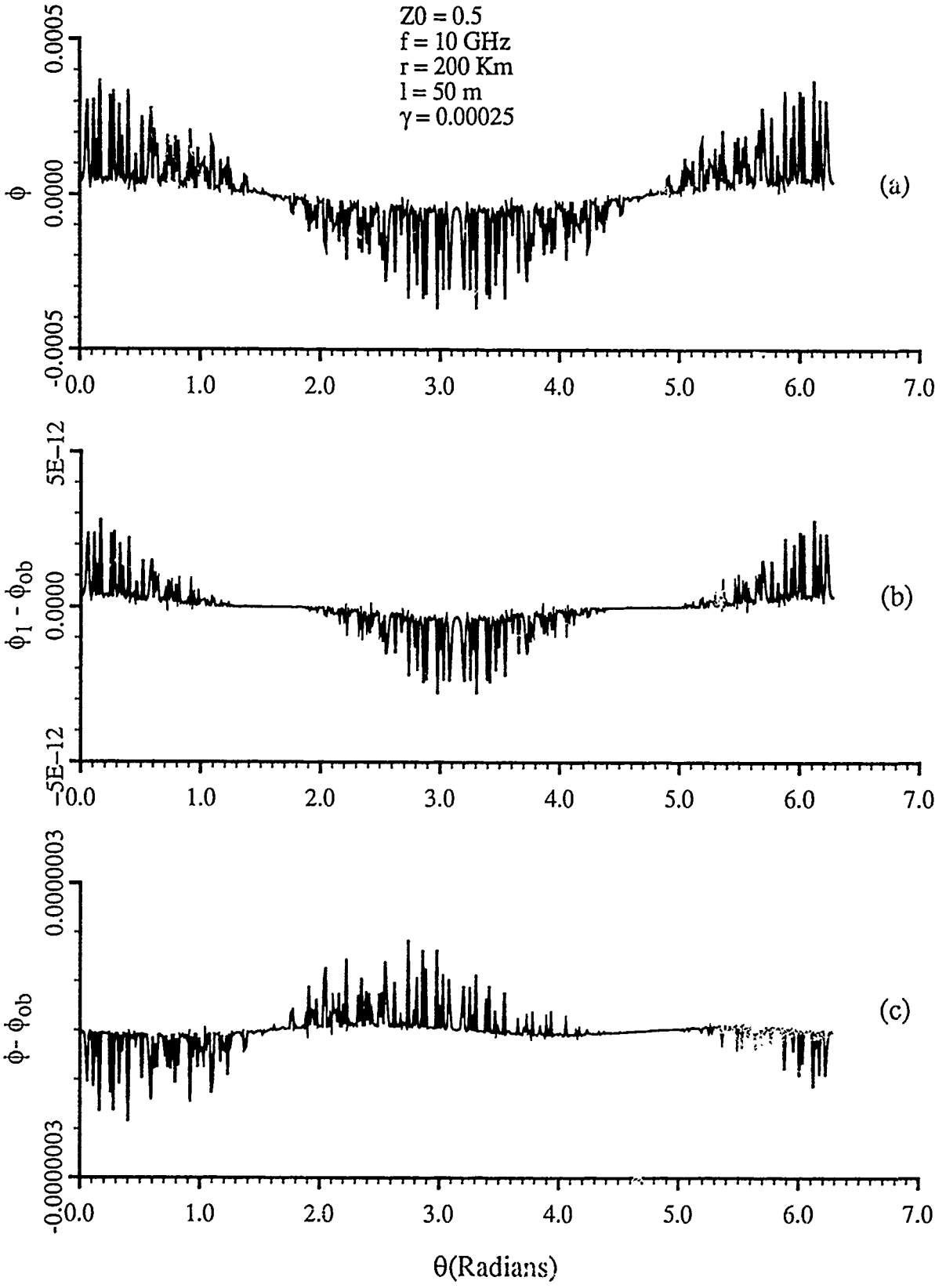

Fig. 7 – Plots of ϕ, $\phi_1 - \phi_{ob}$, and $\phi - \phi_{ob}$ versus θ, all of which are in radians

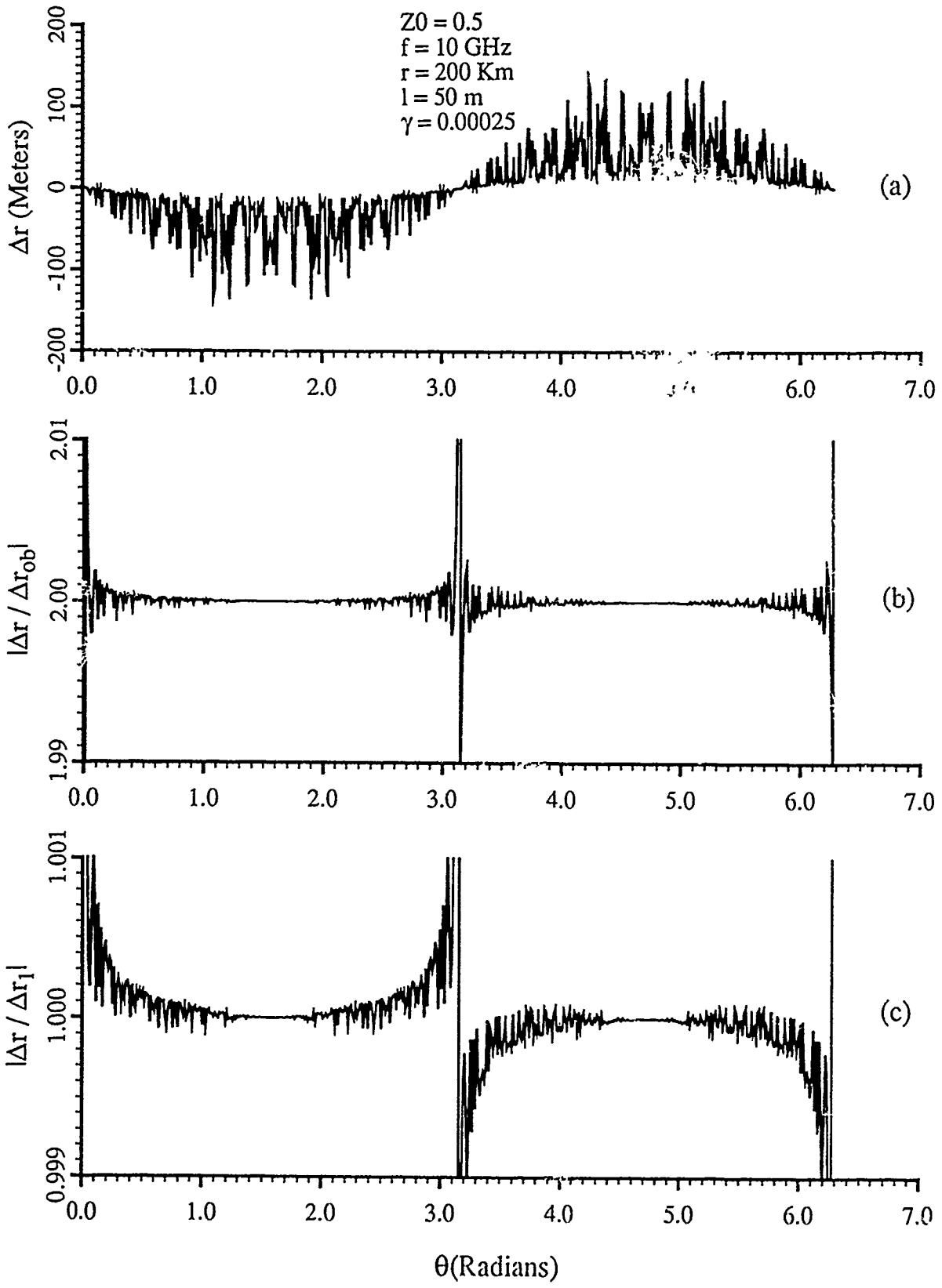

Fig. 8 – Plots of Δr, $|\Delta r / \Delta r_{ob}|$, and $|\Delta r / \Delta r_1|$ versus θ

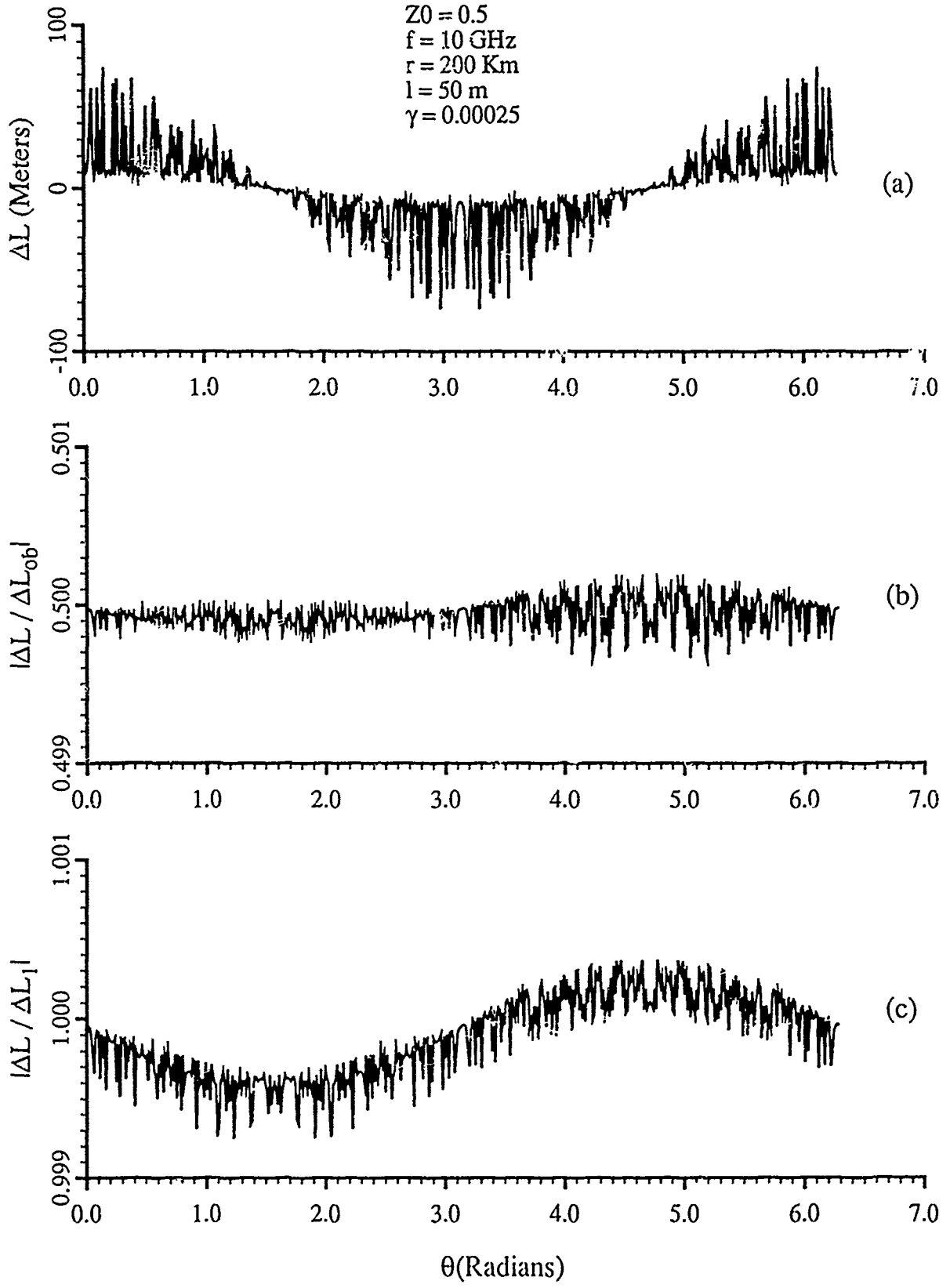

Fig. 9 – Plots of ΔL, $|\Delta L / \Delta L_{ob}|$, and $|\Delta L / \Delta L_1|$ versus θ

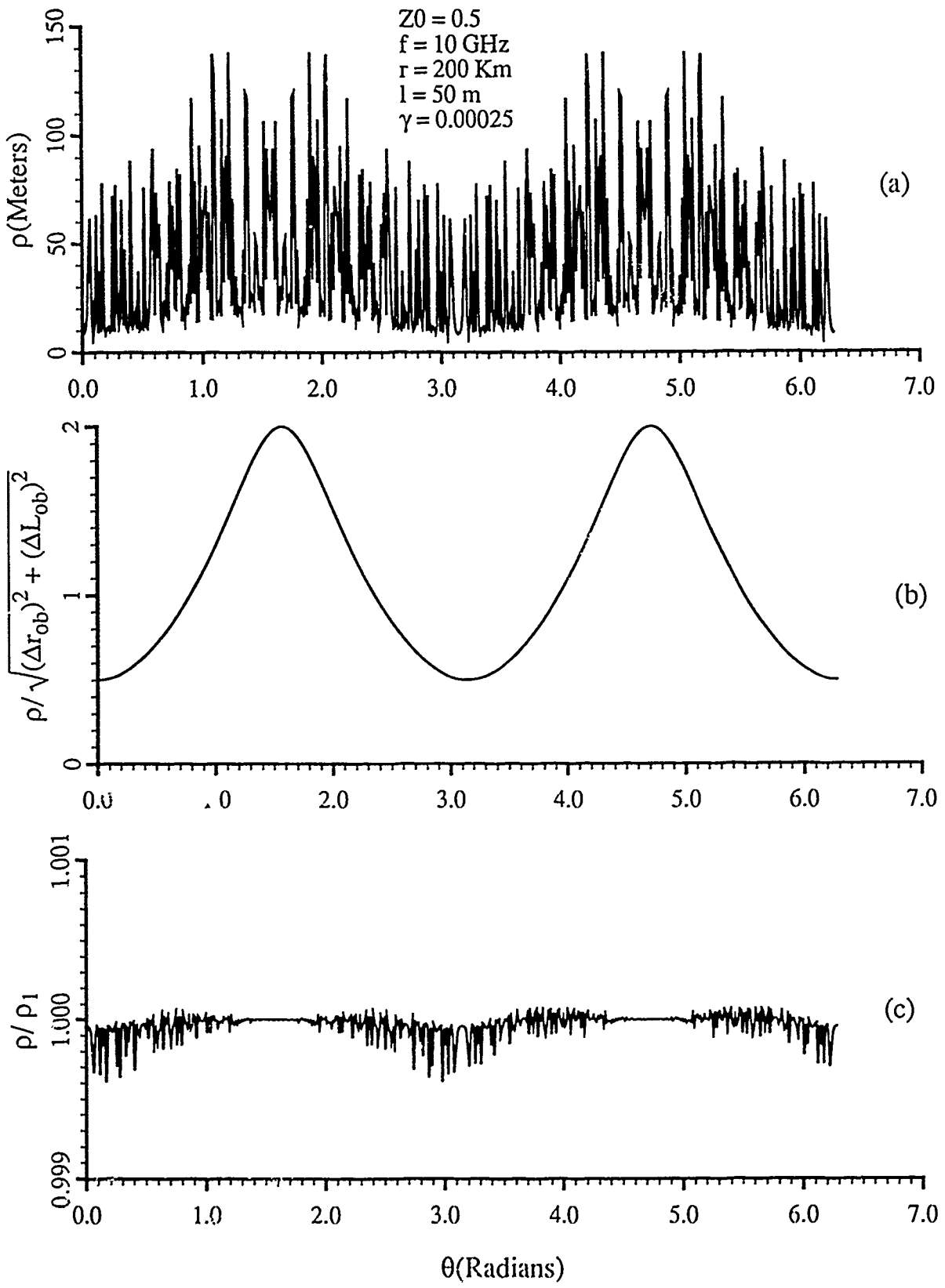

Fig. 10 – Plots of the magnitude of the vector error of the measured position relative to the actual position and of the ratios between the magnitude and two approximations to it

6. LIMITS OF THE RATIO OF THE RANGE ERRORS

To address the issue of whether the approximations converge to the transverse and radial errors, analytical expressions for $\Delta r/\Delta r_1$, $\Delta r/\Delta_{ob}$, $\Delta L/\Delta L_1$, and $\Delta L/\Delta L_{ob}$ are now considered for $\delta_2 - \delta_1 = 0$. Evaluation of the limits of these quotients as γ approaches zero for fixed θ is treated first. Then the limits as θ approaches 0, π, and 2π for fixed γ are evaluated because the ratios may be zero or may not exist. The behavior at these specific θ for small γ are then determined by taking a second limit as γ approaches zero.

Equations (20), (23), (24), and (28) yield

$$\frac{\Delta L}{\Delta L_1} = \frac{\sin\phi}{\sin\phi_1}\left\{1 + \frac{\gamma^2}{8}\cos^2\theta + O(\gamma^4) + \left[\gamma\sin\theta - \frac{\gamma^3}{8}\sin\theta\cos^2\theta + O(\gamma^4)\right] \times \frac{1 - z_0^2}{z_0^2 + 1 + 2z_0\cos\left[(2\omega r/c)\left(\gamma\sin\theta - \frac{\gamma^3}{8}\sin\theta\cos^2\theta + O(\gamma^4)\right)\right]}\right\} \div \left\{1 + \gamma\sin\theta\frac{1 - z_0^2}{z_0^2 + 1 + 2z_0\cos\left[(2\omega r\gamma/c)\sin\theta\right]}\right\}, \tag{30(a)}$$

$$\frac{\Delta r}{\Delta r_1} = \left\{1 - \cos\phi\left(1 + \frac{\gamma^2}{8}\cos^2\theta + O(\gamma^4) + \left[\gamma\sin\theta - \frac{\gamma^3}{8}\sin\theta\cos^2\theta + O(\gamma^4)\right] \times \frac{1 - z_0^2}{z_0^2 + 1 + 2z_0\cos\left[(2\omega r/c)\left(\gamma\sin\theta - \frac{\gamma^3}{8}\sin\theta\cos^2\theta + O(\gamma^4)\right)\right]}\right)\right\} \div \left\{1 - \cos\phi_1\left(1 + \gamma\sin\theta\frac{1 - z_0^2}{z_0^2 + 1 + 2z_0\cos\left[(2\omega r\gamma/c)\sin\theta\right]}\right)\right\}, \tag{30(b)}$$

$$\frac{\Delta L}{\Delta L_{ob}} = \sin\phi\left\{1 + \frac{\gamma^2}{8}\cos^2\theta + O(\gamma^4) + \left[\gamma\sin\theta - \frac{\gamma^3}{8}\sin\theta\cos^2\theta + O(\gamma^4)\right] \times \frac{1 - z_0^2}{z_0^2 + 1 + 2z_0\cos\left[(2\omega r/c)\left(\gamma\sin\theta - \frac{\gamma^3}{8}\sin\theta\cos^2\theta + O(\gamma^4)\right)\right]}\right\} \div \left\{\gamma\cos\theta\frac{1 - z_0^2}{z_0^2 + 1 + 2z_0\cos\left[(2\omega r\gamma/c)\sin\theta\right]}\right\}, \tag{30(c)}$$

$$\frac{\Delta r}{\Delta r_{ob}} = \left\{1 - \cos\phi\left(1 + \frac{\gamma^2}{8}\cos^2\theta + O(\gamma^4) + \left[\gamma\sin\theta - \frac{\gamma^3}{8}\sin\theta\cos^2\theta + O(\gamma^4)\right] \times \frac{1 - z_0^2}{z_0^2 + 1 + 2z_0\cos\left[(2\omega r/c)\left(\gamma\sin\theta - \frac{\gamma^3}{8}\sin\theta\cos^2\theta + O(\gamma^4)\right)\right]}\right)\right\} \div \left\{-\frac{\gamma\sin\theta}{2}\frac{1 - z_0^2}{z_0^2 + 1 + 2z_0\cos\left[(2\omega r\gamma/c)\sin\theta\right]}\right\}. \tag{30(d)}$$

Observe that

$$\lim_{\gamma\to 0}\phi = 0, \qquad \lim_{\gamma\to 0}\phi_1 = 0, \qquad \lim_{\gamma\to 0}\frac{\tan\phi}{\tan\phi_1} = 1; \tag{31}$$

and consequently

$$\lim_{\gamma\to 0}\frac{\phi}{\phi_1} = \lim_{\gamma\to 0}\frac{\sin\phi}{\sin\phi_1} = 1. \tag{32}$$

From Eqs. (30(a)), (30(b)), (31), and (32), it follows that

$$\lim_{\gamma\to 0}\frac{\Delta L}{\Delta L_1} = 1 \qquad \text{and} \qquad \lim_{\gamma\to 0}\frac{\Delta r}{\Delta r_1} = 1. \tag{33}$$

To determine the limit of Eq. (30(d)), an interim approximation of $\Delta r/\Delta r_{ob}$ is now obtained. For small γ, $\cos\phi$ may be replaced by unity. In addition, all terms with γ raised to a power exceeding one are eliminated. Thus, Eq. (30(d)) becomes

$$\frac{\Delta r}{\Delta r_{ob}} \simeq \left\{ r - \left\{ r + r\gamma\sin\theta \frac{1-z_0^2}{z_0^2+1+2z_0\cos\left[(2\omega r\gamma/c)(\sin\theta)\right]} \right\} \right\} \div \left\{ -\frac{r\gamma\sin\theta}{2}\frac{1-z_0^2}{z_0^2+1+2z_0\cos\left[(2\omega r\gamma/c)\sin\theta\right]} \right\}, \tag{34}$$

from which

$$\lim_{\gamma\to 0}\frac{\Delta r}{\Delta r_{ob}} = 2. \tag{35}$$

Next consider

$$\frac{\Delta L}{\Delta L_{ob}} = \frac{\sin\phi}{\gamma\cos\theta}\frac{z_0^2+1+2z_0\cos\left[(2\omega r\gamma/c)\sin\theta\right]}{1-z_0^2} \times \left\{ 1 + \frac{\gamma^2}{8}\cos^2\theta + O(\gamma^4) + \left[\gamma\sin\theta - \frac{\gamma^3}{8}\sin\theta\cos^2\theta + O(\gamma^4)\right] \times \cos\theta\frac{1-z_0^2}{z_0^2+1+2z_0\cos\left[(2\omega r\gamma/c)\sin\theta\right]} \right\}. \tag{36}$$

The bracketed expression to the right of the first times sign goes to unity as $\gamma \to 0$; so it remains to ascertain the behavior of the term involving ϕ. In particular, for small γ (and hence small ϕ), $\sin\phi$ is replaced by $\tan\phi$, Eq. (20(a)) is applied, and the limit is evaluated to obtain

$$\lim_{\gamma\to 0}\frac{\Delta L}{\Delta L_{ob}} = \lim_{\gamma\to 0}\frac{\sin\phi}{\gamma\cos\theta}\frac{z_0^2+1+2z_0\cos\left[(2\omega r\gamma/c)\sin\theta\right]}{1-z_0^2} = \frac{1}{2}. \tag{37}$$

The behavior of the quotients in Eqs. (30) for θ equal to 0, π, and 2π are now determined by evaluating the limits as θ approaches these values and taking the resultant limits, if possible, as γ approaches zero.

For fixed γ,

$$\lim_{\theta\to 0,\pi,2\pi}\frac{\Delta r}{\Delta r_1} = \frac{\sqrt{1+\frac{\gamma^2}{4}\frac{(1-z_0)^2}{(1+z_0)^2}} - \sqrt{1+\frac{\gamma^2}{4}}}{\sqrt{1+\frac{\gamma^2}{4}\frac{(1-z_0)^2}{(1+z_0)^2}} - 1}, \tag{38}$$

for $z_0 \neq 1$, which leads to

$$\lim_{\gamma \to 0} \left\{ \lim_{\theta \to 0,\pi,2\pi} \frac{\Delta r}{\Delta r_1} \right\} = 1 - \left(\frac{1+z_0}{1-z_0} \right)^2 . \tag{39}$$

Clearly this expression has an infinite discontinuity at $z_0 = 1$. Thus as z_0 approaches unity, the limit of the absolute value of $\Delta r/\Delta r_1$ tends to positive infinity.

Letting $z_0 = 0.5$ in Eq. (39) yields 8 for the absolute value of this double limit. Upon inspection of Figs. 4(c) and 8(c), one can see that the analytical and graphical results are in agreement for θ equal 0, π, and 2π.

In comparison, the limits of $\Delta r/\Delta r_{ob}$ as θ approaches 0, π, and 2π do not exist since

$$\lim_{\theta \to 0,\pi,2\pi} \Delta r_{ob} = 0 \qquad \text{and} \qquad \lim_{\theta \to 0,\pi,2\pi} \Delta r = r \left\{ 1 - \frac{\sqrt{1+\frac{\gamma^2}{4}}}{\sqrt{1+\frac{\gamma^2}{4}\frac{(1-z_0)^2}{(1+z_0)^2}}} \right\}; \tag{40}$$

but in the extended real numbers,

$$\lim_{\theta \to 0,\pi,2\pi} \left| \frac{\Delta r}{\Delta r_{ob}} \right| = +\infty. \tag{41}$$

This is exhibited in Figs. 4(b) and 8(b), where the curves have sharp jumps at θ equal 0, π, and 2π. These jumps are similar to those of Figs. 4(c) and 8(c), except that in the present case, instead of finite values for the functic .t these θ, the functions are undefined and have vertical asymptotes.

The expressions for the ratios of the transverse errors are a bit simpler. More specifically,

$$\lim_{\theta \to 0,\pi,2\pi} \frac{\Delta L}{\Delta L_1} = \sqrt{1+\frac{\gamma^2}{4}} \qquad \text{and} \qquad \lim_{\theta \to 0,\pi,2\pi} \frac{\Delta L}{\Delta L_{ob}} = \frac{1}{2} \frac{\sqrt{1+\frac{\gamma^2}{4}}}{\sqrt{1+\frac{\gamma^2}{4}\frac{(1-z_0)^2}{(1+z_0)^2}}}, \tag{42}$$

where Eqs. (42) are valid for all positive z_0. Hence

$$\lim_{\gamma \to 0} \left\{ \lim_{\theta \to 0,\pi,2\pi} \frac{\Delta L}{\Delta L_1} \right\} = 1 \qquad \text{and} \qquad \lim_{\gamma \to 0} \left\{ \lim_{\theta \to 0,\pi,2\pi} \frac{\Delta L}{\Delta L_{ob}} \right\} = \frac{1}{2}. \tag{43}$$

In general, as γ decreases to zero, all errors become smoother, the first-order approximations approach the actual errors, and Δr_{ob} and ΔL_{ob} approach $\Delta r/2$ and $2\Delta L$, respectively, except near θ equal to 0, π, and 2π. Hence ΔL_{ob} is eventually an upper bound for ΔL so that the transverse error is less than ΔL_{ob}. On the other hand, Δr_{ob} is double the actual radial range error for very small γ. Therefore Δr_{ob} and ΔL_{ob} are not good estimates Δr and ΔL for small γ and θ not near 0, π, and 2π; however, the relationships among them are precisely known.

All of these analytically derived conclusions about the behavior of the two sets of approximations for small γ can be seen in Figs. 7 through 10. The first-order approximation to the transverse range error ΔL is excellent (Fig. 9(c), Eq. (33)), even for θ near 0, π, 2π (Eq. (43)). The radial range error Δr_1 closely approximates Δr (Fig. 8(c)) except near 0, π, 2π, where the ratio increases to a finite, nonzero value in accordance with Eqs. (33) and (39). Lastly, the predicted relationships (Eqs. (35), (37), (41), (42)) between the approximations of Ref. 1 and the exact range errors are displayed in Figs. 8(b) and 9(b).

Generally it turns out that the first-order approximations of the range errors are excellent for $\gamma \in [0, 0.000001]$, are good for $\gamma \in (0.000001, 0.0003]$, are fair for $\gamma \in (0.0003, 0.005]$, and are poor for $\gamma \in (0.005, 1.0]$. Appropriate multiples of the range estimates of Ref. 1 behave similarly. Also both approximations to the angular error are accurate for γ smaller than 0.005.

7. SUMMARY

Based on the assumption that the measured centroid of a two-point target is determined from the phase ψ_S of the composite signal of the individual returns, exact expressions for the angular, transverse range, radial range, and vector errors have been derived. These errors depend on six parameters: the transmission frequency ($2\pi f = \omega$); the range to the centroid of the two scatterers (r); the difference between the phases induced by each scatterer ($\delta_2 - \delta_1$); the ratio of the amplitudes of the individual scatterers (z_0); the angle between the line segment from the centroid to the radar and the perpendicular bisector of the line segment connecting the scatterers (θ); and the ratio of the distance between the scatterers to the centroidal range (γ).

Examples are analyzed for specific choices of f, z_0, and $\delta_2 - \delta_1$ (10 GHz, 0.5, and 0 rad). Two conclusions can be drawn from this analysis. First, the magnitude of the vector error the distance between the measured and actual target centroids can be large even for small values of γ. In one example where $\gamma = 0.00025$, this error is three times the distance between the scatterers for some target orientations, which means the measured target location could be off by three body lengths. Consequently, the measured location can be well away from the actual target.

Second, approximate formulae for the angular and range errors, such as the far field approximation to the geometry, should not be used in place of exact expressions without proper consideration of the errors incurred by their use. It has been demonstrated that such approximations can diverge substantially from the actual errors. In particular, the formulae of Ref. 1 may not be adequate for representing the radial and transverse range errors when $\gamma > 0.00025$, since these estimates of the errors are twice and one half the real values, respectively, for small γ, while the first-order approximations derived herein are inaccurate for γ in excess of 0.005. Therefore when $\gamma > 0.005$, exact expressions or more accurate approximations for the errors must be used if one wishes to get an accurate assessment of the range and angular errors. On the other hand, for $\gamma < 0.005$, the first-order approximations are valid. Even the radial and transverse range errors of Ref. 1 can be used, provided their relationships to the actual range errors are kept in mind. Although a three dimensional analysis both for two point and N point targets would be more realistic, this two-dimensional analysis provides additional insight into the glint problem.

This analysis indicates that the glint phenomena may be caused in part by the inherent error in the positional measurement. If this error is deemed significant and is attributable to a theoretical formulation that resulted in the equations specifying position, then the theory should be revamped to account for this. Even if the existing theory is correct, an explanation of this error should be sought. The situation is complicated further by the introduction of an additional error through approximations to the theoretical expressions for the position. Whether the combination of the inherent and approximation induced errors reduces or increases the measured positional error is unclear. In terms of application to a radar system, errors of the magnitudes demonstrated herein may be significant. For example, a 4° angular error for an incoming object could be very important.

8. REFERENCES

1. R. V. Ostrovityanov and F. A. Basalov, *Statistical Theory of Extended Radar Targets* (Artech House, Dedham, MA, 1985).

2. J. H. Dunn, D. D. Howard, and A. M. King, "Phenomena of Scintillation Noise in Radar Tracking Systems," *Proc. IRE* 47(5), 855-863 (1959).

3. D. D. Howard, "Radar Target Angular Scintillation in Tracking and Guidance Systems Based on Echo Signal Phase Front Distortion," Proceedings of the National Electronics Conference, 13-15 October 1959, Hotel Sherman, Chicago, Illinois.

4. L. A. Wainstein and V. D. Zubakov, *Extraction of Signals from Noise*, Moscow: Soviet Radio (1960), translated by R. A. Silverman (Prentice-Hall, Englewood Cliffs, New Jersey, 1962).

5. S. G. Zubkovich, *Statistical Characteristics of Radio Signals Reflected from the Ground*, Moscow: Soviet Radio, 1968.

6. L. Peters and F. C. Weimer, "Radar Tracking of Complex Targets," *Proc. IEE* **110** (12), 2149–2162 (1963).

7. R. H. Delano, "A Theory of Target Glint or Angular Scintillation in Radar Tracking," *Proc. IRE* **41** (12), 1778–1784 (1953).

8. A. S. Locke, *Guidance* (Van Nostrand Reinhold, New York, 1955).

9. L. Peters and F. C. Weimer, "Concerning the Assumption of Random Distribution of Scatterers as a Model of an Aircraft for Tracking Radars," *IRE Trans. on Ant. and Prop.* **AP-9** (1), 110–111 (1961).

10. Ya. D. Shirman and V. N. Golikov, "On the Theory of Straying of the Effective Center of Secondary Emission," *Radio Engineering and Electronic Physics* **13** (11), 1821–1823 (1968).

11. J. V. Lindsay, "Angular Glint and the Moving, Rotating, Complex Radar Target," *IEEE Trans. Aerospace and Electronic Sys.* **AES-4** (2), 164–173 (1968).

12. K. C. Yeh and C. H. Liu, *Theory of Ionospheric Waves* (Academic Press, New York, 1972).